Ulnar collateral ligament dysfunction increases stress on the humeral capitellum: a finite element analysis

Keita Kamei, MD [a,*], Eiji Sasaki, MD, PhD [a], Kazuhiro Fujisaki, PhD [b],
Yoshifumi Harada, MD, PhD [a], Yuji Yamamoto, MD, PhD [a], Yasuyuki Ishibashi, MD, PhD [a]

[a] Department of Orthopaedic Surgery, Hirosaki University Graduate School of Medicine, Hirosaki, Japan
[b] Department of Intelligent Machines and System Engineering, Faculty of Science and Technology, Hirosaki University, Hirosaki, Japan

Background: Repetitive mechanical stress on the elbow joint during throwing is a cause of ulnar collateral ligament dysfunction that may increase the compressive force on the humeral capitellum. This study aimed to examine the effects of ulnar collateral ligament material properties on the humeral capitellum under valgus stress using the finite element method.

Methods: Computed tomography data of the dominant elbow of five healthy adults were used to create finite element models. The elbows were kept at 90° of flexion with the forearm in the neutral position, and the ulnar collateral ligament was reproduced using truss elements. The proximal humeral shaft was restrained, and valgus torque of 40 N·m was applied to the forearm. The ulnar collateral ligament condition was changed to simulate ulnar collateral ligament dysfunction. Ulnar collateral ligament stiffness values were changed to 72.3 N/mm, 63.3 N/mm, 54.2 N/mm, 45.2 N/mm, and 36.1 N/mm to simulate ulnar collateral ligament laxity. The ulnar collateral ligament toe region width was changed in increments of 0.5 mm from 0.0 to 2.5 mm to simulate ulnar collateral ligament loosening. We assessed the maximum equivalent stress and stress distribution on the humeral capitellum under these conditions.

Results: As ulnar collateral ligament stiffness decreased, the maximum equivalent stress on the humeral capitellum gradually increased under elbow valgus stress ($P < .001$). Regarding the change in the ulnar collateral ligament toe region width, as the toe region elongated, the maximum equivalent stress of the humeral capitellum increased significantly under elbow valgus stress ($P < .001$). On the capitellum, the equivalent stress on the most lateral part was significantly higher than that on other parts ($P < .01$ for all).

Conclusion: Under elbow valgus stress with elbow flexion of 90° and the forearm in the neutral position, ulnar collateral ligament dysfunction increased equivalent stress on the humeral capitellum during the finite element analysis. The highest equivalent stress was noted on the lateral part of the capitellum.

The ulnar collateral ligament (UCL) is the primary restraint of elbow valgus stress, and repetitive throwing motions could cause microscopic tearing and rupture.[1,13] Poor biomechanics of throwing, fastball velocity, and in-season workload are considered risk factors for UCL injury in adolescent and adult baseball players.[5,7,8,30] Regarding juvenile baseball players, Matsuura et al[19] reported that 137 of 449 (30.5%) players aged 7-11 years had episodes of elbow pain, especially on the medial side, and 68 of 86 (79.1%) players who underwent radiographic evaluation exhibited medial epicondylar fragmentation. Previous studies showed that repetitive throwing motions and fatigue of the forearm flexion muscles cause elbow medial joint laxity.[12,25]

Osteochondritis dissecans (OCD) of the humeral capitellum is also a common disease observed in juvenile baseball players. Repetitive compression and shear forces to the capitellum during the throwing motion might be pathological factors.[38] When the elbow was flexed 95° ± 14° during the late cocking phase or acceleration phase, maximum varus torque of the elbow joint was produced.[8] Funakoshi et al[9] analyzed stress distribution in baseball pitchers aged 17-24 years using computed tomography (CT) osteoabsorptiometry. They reported that pitchers who had symptomatic valgus instability with UCL insufficiency had high-stress distribution patterns on the anterolateral part of the capitellum. This indicated that repetitive pitching motions with medial joint laxity could increase the stress of the humeral capitellum. This study shows the

long-term stress distribution patterns of the pitching motion; however, the mechanism of medial joint laxity increasing the stress of the humeral capitellum was not clearly understood.

The finite element (FE) method is used for analyzing initial stress distribution and the failure prediction of materials. It is mainly used in the material and industrial engineering fields; however, it is also applied in the medical field, especially in orthopedics.[22,26] The FE method shows the single-load condition of the material, which could help clarify mechanisms and biomechanics. Several studies using the FE method to assess the elbow joint have been reported.[23,27,39] However, these reports did not assess changes in UCL material properties. Therefore, because the UCL is resistant to valgus stress, we considered the UCL material properties during a study of the elbow joint involving the FE method.

This study aimed to examine the effects of UCL material properties on the humeral capitellum under valgus stress using the FE method. We considered that UCL laxity could be simulated by changing the UCL stiffness and that UCL loosening could be simulated by changing the UCL toe region width, which represents alignment and tension of the UCL. Our hypothesis was that changes in the UCL stiffness and toe region width affect the equivalent stress of the humeral capitellum under valgus stress.

Materials and methods

Data collection

Dominant elbow CT data were collected from five healthy male volunteers with a mean age of 27.6 years (range, 26-29 years). None of the participants had symptoms in the elbow or a history of elbow trauma. All participants had a history of participating in non-throwing sports. CT was performed with the following imaging parameters: 320-row detector; 120 kV; 200 mA; slice thickness, 0.625 mm; and pixel width, 0.3 mm (Discovery 750 HD system; GE Healthcare, Chicago, IL, USA). During CT, the elbow was kept at 90° of flexion with the forearm in the neutral position; this simulated the arm position of the acceleration phase of the pitching motion. CT data of all 5 aforementioned parameters were used in the FE analysis. The study design was approved by our institution's ethics committee, and all patients provided informed written consent before inclusion in the study.

FE method

Model development

The CT data were transferred to the workstation (ThinkStation P500; Lenovo, Morrisville, NC, USA). The elbow model was made using FE method software (Mechanical Finder; Research Center for Computational Mechanics, Tokyo, Japan). A humeral bone model was created from the distal two-thirds of the humerus. Forearm bone models were created from the proximal two-thirds and constrained at one-half the forearm length with a rectangular model to imitate fixation of the distal forearm for convenient load application. Cartilage was reproduced to enlarge the subchondral bone to 2 mm. The gap element was configured on the ulnar cartilage part to remove the tensile force of the humeroulnar joint. Only the anterior oblique ligament of the UCL was simulated with truss elements. The trabecular bone and cortex were meshed using linear tetrahedral elements with a 2- to 4-mm global edge length overlaid with $2 \times 2 \times 0.01$-mm triangular shell elements simulating the outer cortex (Figure 1).

Material properties

The CT values of each element were set as the mean of the voxels contained in one element. The mechanical properties of each
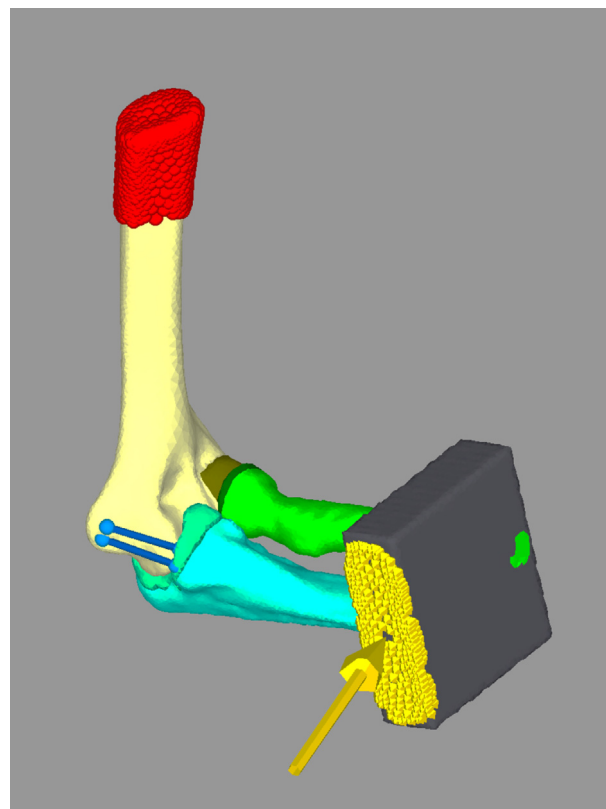

Figure 1 Finite element model of the elbow. An anterior oblique bundle of the ulnar collateral ligament (UCL) was simulated by truss elements (*blue lines*). The proximal humerus was constrained (*red zone*). The radius and ulna were fixed by the rectangular block (*black box*) on which valgus torque was applied (*yellow arrow*).

element were calculated in Hounsfield units (HU). Regarding the bone materials, Young's modulus and Poisson's ratio were calculated from the HU using the expression of Keyak.[14] The material properties of cartilage were modeled as an elastic material with a Young's modulus of 10 MPa and Poisson's ratio of 0.49.[6,10,21] The rectangular model that constrained the middle of the forearm was given the material properties of dry resin (Young's modulus, 3724 MPa; Poisson's ratio, 0.4).

The truss elements with deformation characteristics in the toe and linear regions were used to represent the elongation behavior of ligaments. To represent the UCL, 0 N/mm was set as the toe region stiffness and 72.3 N/mm was set as the linear region stiffness for the truss elements of the medial elbow.[23] To create the UCL dysfunction model, we changed the material properties of the truss elements to mimic the UCL conditions (Figure 2).[10,31,36] To mimic decreasing UCL stiffness as UCL laxity, one-half, five-eighths, three-fourths, and seven-eighths of normal UCL material property were calculated and those values were used. The stiffness values of the truss element were changed to 72.3, 63.3, 54.2, 45.2, and 36.1 N/mm with the toe region set at 0 mm. According to a study that examined the medial gap using ultrasonography, the medial joint gap at gravity stress before throwing was 5.0 mm at 90° of elbow flexion, whereas the medial gap at gravity stress after 100 pitches was 6.2 mm and the gap under 30 N of valgus stress was 7.0 mm.[12] Based on these results, it was considered sufficient to examine medial joint loosening of approximately 2 mm. Therefore, the study focused on the toe region from 0 mm to 2.5 mm. Then, the toe region width was changed from 0.0 to 2.5 mm in 0.5-mm increments to simulate UCL loosening, with UCL stiffness set at 72.3 N/mm.

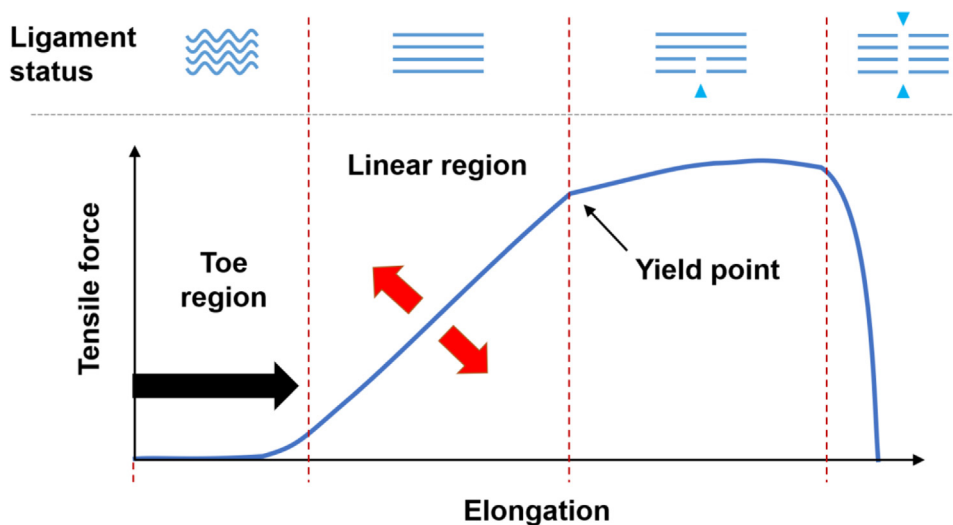## Schematic diagram of UCL dysfunction model

Figure 2 Ulnar collateral ligament (UCL) dysfunction model. A schematic diagram of the tensile-elongation curve and ligament status are shown.[10,31,36] UCL laxity was simulated by changing the UCL stiffness (➡). UCL loosening was simulated by changing the UCL toe region width (➡).

Measurement

The proximal humeral shaft was restrained, and the valgus force load was applied to the rectangular model of the forearm from the ulnar side to simulate valgus stress during the pitching motion. The valgus load was calculated so that the torque applied to the elbow joint was 40 N·m. The equivalent stress of the humeral capitellum was measured, and the maximum equivalent stress and area were identified for analysis. To analyze the medial-lateral stress distribution patterns, we divided the humeral capitellum into 4 parts—medial (part A), central-medial (part B), central-lateral (part C), and lateral (part D)—and we measured the mean equivalent stress of every part (Figure 3). Five models were used to analyze all these situations, and the data were collected.

Statistical analysis

The maximum or mean equivalent stress values of the 5 cases are expressed as means ± standard deviations. The effects of UCL stiffness and the UCL toe region width among the humeral capitellum were investigated using Friedman's test. To compare the differences in the maximum stress and mean equivalent stress in each location (medial, central-medial, central-lateral, and lateral), one-way analysis of variance and Tukey's honestly significant difference test as post hoc analyses were performed. The level of significance was set at $P < .05$. All statistical data were analyzed using SPSS, version 22 (IBM, Armonk, NY, USA).

Results

Regarding the changes in UCL stiffness, lower UCL stiffness significantly increased the maximum equivalent stress on the humeral capitellum under elbow valgus stress (Figure 4a). The mean maximum equivalent stress values of the humeral capitellum were 155.3 ± 24.2, 160.2 ± 24.2, 166.2 ± 24.1, 173.8 ± 23.8, and 183.9 ± 23.4 MPa with the stiffness of the UCL set at 72.3 N/mm, 63.3 N/mm, 54.2 N/mm, 45.2 N/mm, and 36.1 N/mm ($P < .001$), respectively. Regarding changes in the UCL toe region, a longer toe region width increased the maximum equivalent stress on the humeral capitellum (Figure 4b). The mean maximum equivalent stress
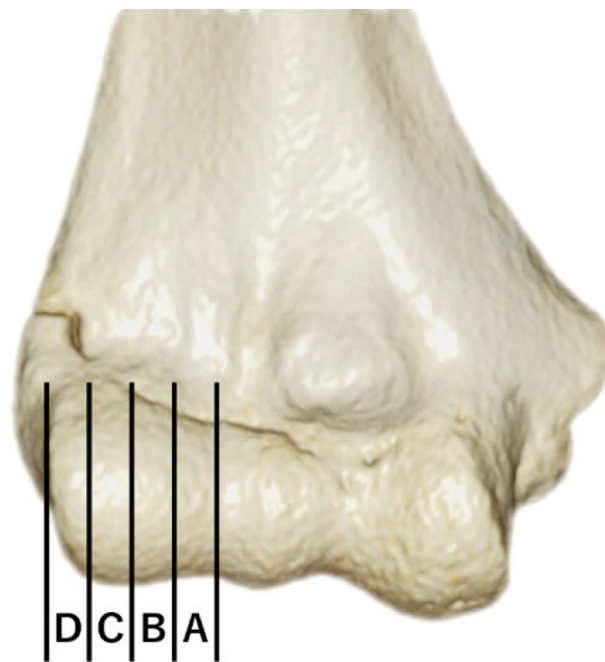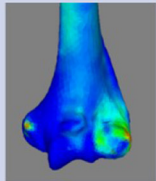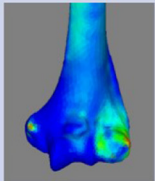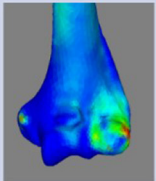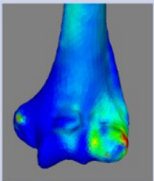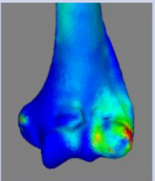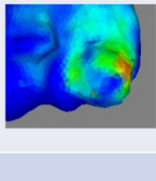

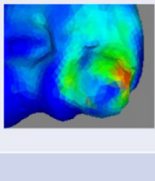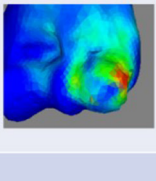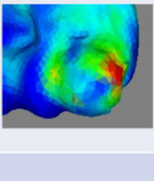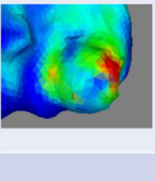**Figure 3** Four areas of the humeral capitellum to assess stress distribution. The humeral capitellum was divided into four parallel parts in the direction of the long axis, from medial to lateral. (A) medial; (B) central-medial; (C) central-lateral; (D) lateral.

values of the humeral capitellum were 155.3 ± 24.2, 159.4 ± 25.7, 161.3 ± 24.6, 163.1 ± 23.4, and 167.3 ± 25.6 MPa with toe region widths of 0.0 mm, 0.5 mm, 1.0 mm, 1.5 mm, 2.0 mm, and 2.5 mm ($P < .001$), respectively.

Regarding the medial-lateral stress distribution, the mean equivalent stress increased in all areas with the decreasing UCL stiffness and with the increasing UCL toe region width (Figure 5). The maximum equivalent stress was noted at the lateral part of the capitellum. The equivalent stress was significantly concentrated on the lateral part in all models ($P < .01$ for all).

a

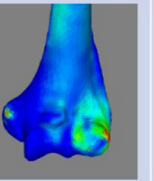| Stiffness (N/mm)	72.3	63.2	54.2	45.2	36.1
Distal of Humerus					
Humeral Capitellum					
Maximum equivalent stress (MPa)	155.3 ± 24.2	160.2 ± 24.2	166.2 ± 24.1	173.8 ± 23.8	183.9 ± 23.4

b
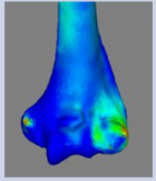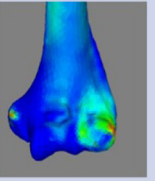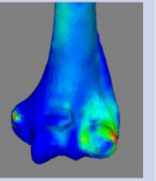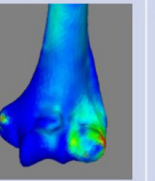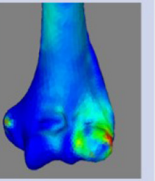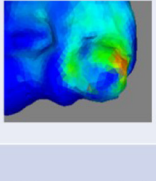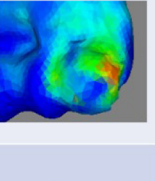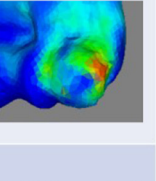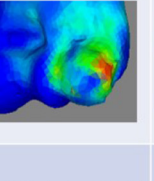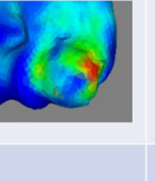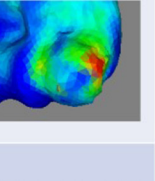
Toe region width (mm)	0.0	0.5	1.0	1.5	2.0	2.5
Distal of Humerus						
Humeral Capitellum						
Maximum equivalent stress (MPa)	155.3 ± 24.2	159.4 ± 25.7	161.3 ± 24.6	163.1 ± 23.4	165.9 ± 23.6	167.3 ± 25.6

Figure 4 Equivalent stress distribution under ulnar collateral ligament (UCL) stiffness and toe region width changes. (**a**) Stiffness changing model. As the UCL stiffness decreased, the maximum equivalent stress of the humeral capitellum significantly increased ($P < .001$). (**b**) The UCL toe region width changing model. As the UCL toe region widened, the maximum equivalent stress of the humeral capitellum significantly increased ($P < .001$).

Discussion

This study showed that the maximum equivalent stress on the humeral capitellum increased under elbow valgus stress as the UCL stiffness decreased. Similarly, the maximum equivalent stress on the humeral capitellum increased when the UCL toe region width widened. The mean equivalent stress on the lateral part was significantly higher than that on other parts of the humerus.

Although the equivalent stress mainly occurred on the lateral humeral capitellum, the stress distribution pattern was not significantly different throughout the changes in the UCL stiffness and toe region width.

The UCL is a primary passive restraint against elbow valgus stress. In adult baseball players, the torque that the elbow joint generates is as high as 64 N·m during the pitching motion. Assuming that the UCL produced half of this valgus torque, the load

a

b
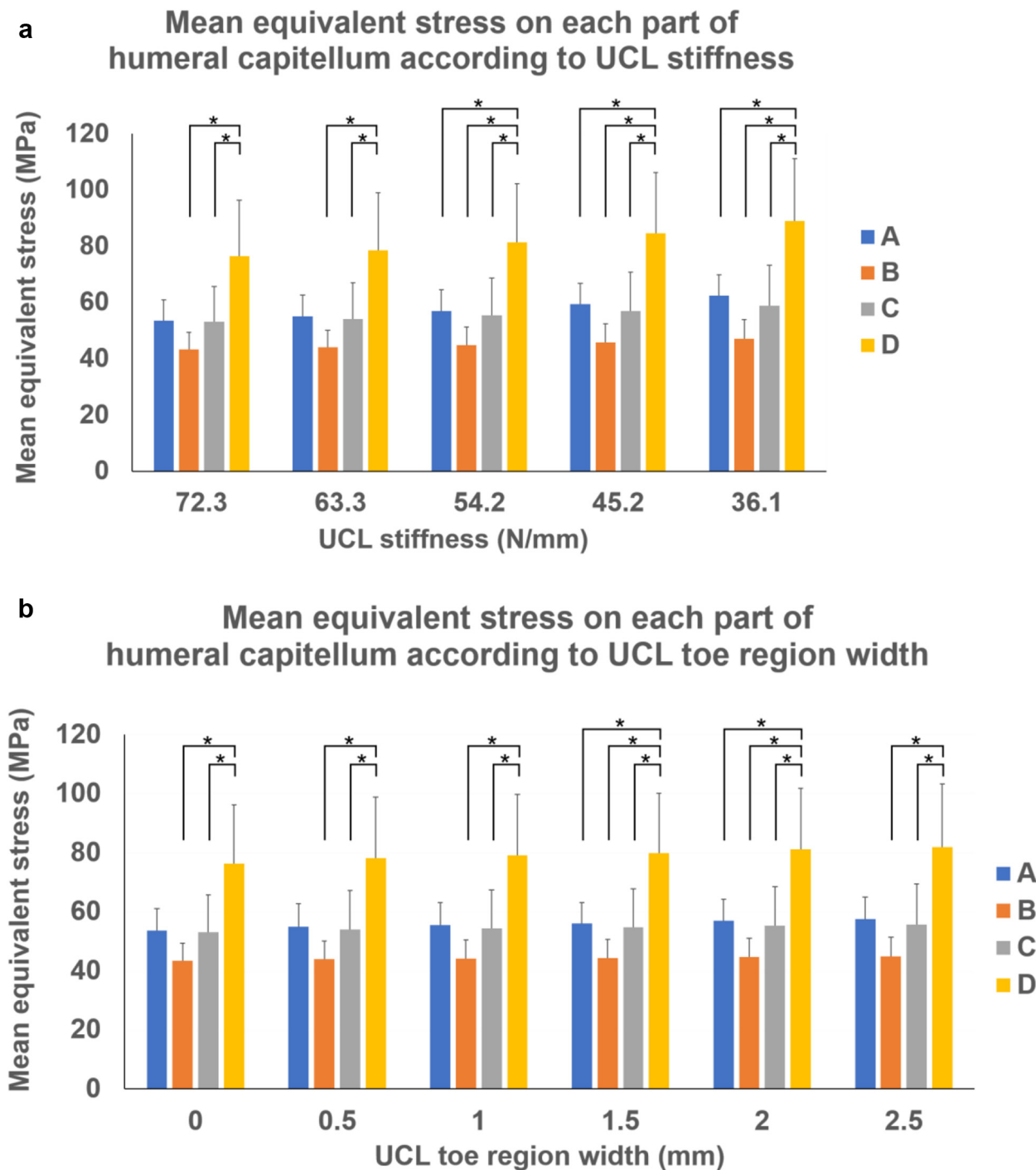
Figure 5 Mean equivalent stress on each part of the humeral capitellum. The mean equivalent stress is shown with the standard deviation. These data were compared using an analysis of variance and Tukey's honestly significant difference test. *P < .05 was statistically significant. (**a**) The mean equivalent stress values with ulnar collateral ligament (UCL) stiffness changes are compared. As the UCL stiffness decreased, the mean equivalent stress of the humeral capitellum increased. Among the parts of the capitellum, the lateral part (C) shows significantly higher equivalent stress (P < .01 for all). (**b**) The mean equivalent stresses occurring with the UCL toe region width changes are compared. As the UCL toe region width increases, the mean equivalent stress of the humeral capitellum increases. Among the parts of the capitellum, the lateral part (D) shows significantly higher equivalent stress (P < .01 for all).

of the UCL might be greater than the failure strength.[8,29] The flexor pronator muscles work as active restraints for elbow valgus stress.[4,33] Some reports suggest that overuse or fatigue of the upper extremity can cause elbow joint laxity. During an ultrasonographic study, Hattori et al[12] reported that the gap of the medial elbow joint space significantly increased after 60 pitches compared with the baseline. Millard et al[25] reported that repeated wrist flexion exercise decreased the stability of the medial elbow. These reports show that fatigue of the forearm flexor muscle decreased the stabilizing function against valgus stress of the medial elbow. Mihata et al[24] showed that elbow valgus torque increased the contact pressure on the radiocapitellar joint during a cadaveric study. Our study

involving the FE method also showed that UCL dysfunction increased the equivalent stress of the radiocapitellar joint.

Although the exact cause of the disorder remains unclear, the causes of OCD are believed to include simple repetitive mechanical trauma, disruption to the blood supply of a small area of subchondral bone, and disruption of endochondral ossification.[2,17,34,35] Previous studies involving ultrasonographic evaluations showed that the prevalence of elbow OCD among adolescent baseball players was 1.3%-3.4%.[11,15,18,32] Elbow valgus stress during the throwing motion causes compression force on the humeral capitellum. During the late cocking and early acceleration phases of throwing, compressive forces are estimated to be as high as 500 N on the radiocapitellar joint.[3,8] Using CT osteoabsorptiometry, Momma et al[28] reported the stress distribution pattern on the humeral capitellum in baseball pitchers and demonstrated the long-term loading conditions of subchondral bone. Their results show that baseball pitching produces excessive/repetitive stress against the anterior part of the capitellum. In this study, the stress distribution was also concentrated in the lateral part of the capitellum under elbow valgus stress.

The natural progression of elbow OCD remains unknown. Takahara et al[37] reported that the initial radiographic appearance of elbow OCD started from the lateral part of the humeral capitellum and that the lesion then enlarged into the central part of the capitellum. Juvenile OCD lesions, especially with an open capitellar growth plate, have the potential to heal conservatively, and the healing process starts from the lateral part of the capitellum.[37] In our study, the stress distribution during the throwing motion was concentrated on the lateral part of the humeral capitellum. If there is repeated valgus stress without nonthrowing management, then the lateral part of the elbow may continue to be stressed. As mentioned, the lateral part of the humeral capitellum may be the starting point of the OCD healing process. The continuity of throwing stress may increase the risk of interference with healing of the lateral part and lead to lateral widespread lesions and poorer predicted outcomes.[16,20]

This study had some limitations. Our FE model reproduced only the anterior oblique bundle of the UCL. The elbow ligaments, such as the posterior oblique bundle of the UCL and the annular ligament, and several muscles around the elbow were not reproduced. A fixed grid was applied to the radiocapitellar joint. These conditions were not representative of a physiological joint situation. Only fixed 90° of elbow flexion was assessed with this model. The throwing motion provides not only compression force but also shear force to the radiocapitellar joint during elbow extension. In the future, the valgus stress load with an extension motion should be simulated. Although OCD occurs in juvenile athletes, the subjects involved in this study were adults. Furthermore, the sample size was only 5.

Conclusion

Under elbow valgus stress with elbow flexion of 90° and the forearm in the neutral position, as the UCL stiffness decreased, the equivalent stress on the humeral capitellum increased. Similarly, as the UCL toe region width increased, the equivalent stress on the humeral capitellum increased under elbow valgus stress. The equivalent stress was concentrated on the lateral part of the humeral capitellum, which is the origin of the healing process; therefore, UCL dysfunction may affect OCD development and progression.

Disclaimer

The authors declare that they have no competing interests.

References

1. Andrews JR, Zarins B, Wilk KE. Injuries in baseball. Philadelphia: Lippincott Raven; 1998 (ISBN No. 978-0781702591).
2. Baker CL III, Romeo AA, Baker CL Jr. Osteochondritis dissecans of the capitellum. Am J Sports Med 2010;38:1917-28. https://doi.org/10.1177/0363546509354969.
3. Cain EL Jr, Dugas JR, Wolf RS, Andrews JR. Elbow injuries in throwing athletes: a current concepts review. Am J Sports Med 2003;31:621-35. https://doi.org/10.1177/03635465030310042601.
4. Davidson PA, Pink M, Perry J, Jobe FW. Functional anatomy of the flexor pronator muscle group in relation to the medial collateral ligament of the elbow. Am J Sports Med 1995;23:245-50.
5. Dun S, Loftice J, Fleisig GS, Kingsley D, Andrews JR. A biomechanical comparison of youth baseball pitches: is the curveball potentially harmful? Am J Sports Med 2008;36:686-92. https://doi.org/10.1177/0363546507310074.
6. Edwards WB, Troy KL. Finite element prediction of surface strain and fracture strength at the distal radius. Med Eng Phys 2012;34:290-8. https://doi.org/10.1016/j.medengphy.2011.07.016.
7. Fleisig GS, Andrews JR, Cutter GR, Weber A, Loftice J, McMichael C, et al. Risk of serious injury for young baseball pitchers: a 10-year prospective study. Am J Sports Med 2011;39:253-7. https://doi.org/10.1177/0363546510384224.
8. Fleisig GS, Andrews JR, Dillman CJ, Escamilla RF. Kinetics of baseball pitching with implications about injury mechanisms. Am J Sports Med 1995;23:233-9.
9. Funakoshi T, Furushima K, Momma D, Endo K, Abe Y, Itoh Y, et al. Alteration of stress distribution patterns in symptomatic valgus instability of the elbow in baseball players: A computed tomography osteoabsorptiometry study. Am J Sports Med 2016;44:989-94. https://doi.org/10.1177/0363546515624916.
10. Goh KL, Listrat A, Béchet D. Hierarchical mechanics of connective tissues: integrating insights from nano to macroscopic studies. J Biomed Nanotechnol 2014;10:2464-507. https://doi.org/10.1166/jbn.2014.1960.
11. Harada M, Takahara M, Sasaki J, Mura N, Ito T, Ogino T. Using sonography for the early detection of elbow injuries among young baseball players. Am J Roentgenol 2006;187:1436-41. https://doi.org/10.2214/AJR.05.1086.
12. Hattori H, Akasaka K, Otsudo T, Hall T, Amemiya K, Mori Y. The effect of repetitive baseball pitching on medial elbow joint space gapping associated with 2 elbow valgus stressors in high school baseball players. J Shoulder Elbow Surg 2018;27:592-8. https://doi.org/10.1016/j.jse.2017.10.031.
13. Jobe FW, Stark H, Lombardo SJ. Reconstruction of the ulnar collateral ligament in athletes. J Bone Joint Surg Am 1986;68:1158-63.
14. Keyak JH, Rossi SA, Jones KA, Skinner HB. Prediction of femoral fracture load using automated finite element modeling. J Biomech 1998;31:125-33.
15. Kida Y, Morihata T, Kotoura Y, Hojo T, Tachiiri H, Sukenari T, et al. Prevalence and clinical characteristics of osteochondritis dissecans of the humeral capitellum among adolescent baseball players. Am J Sports Med 2014;42:1963-71. https://doi.org/10.1177/0363546514536843.
16. Kosaka M, Nakase J, Takahashi R, Toratani T, Ohashi Y, Kitaoka K, et al. Outcomes and failure factors in surgical treatment for osteochondritis dissecans of the capitellum. J Pediatr Orthop 2013;33:719-24. https://doi.org/10.1097/BPO.0b013e3182924662.
17. Kusumi T, Ishibashi Y, Tsuda E, Kusumi A, Tanaka M, Sato F, et al. Osteochondritis dissecans of the elbow: histopathological assessment of the articular cartilage and subchondral bone with emphasis on their damage and repair. Pathol Int 2006;56:604-12. https://doi.org/10.1111/j.1440-1827.2006.02015.x.
18. Matsuura T, Hashimoto Y, Nishino K, Nishida Y, Takahashi S, Shimada N. Comparison of clinical and radiographic outcomes between central and lateral lesions after osteochondral autograft transplantation for osteochondritis dissecans of the humeral capitellum. Am J Sports Med 2017;45:3331-9. https://doi.org/10.1177/0363546517730358.
19. Matsuura T, Suzue N, Iwame T, Nishio S, Sairyo K. Prevalence of osteochondritis dissecans of the capitellum in young baseball players: Results based on ultrasonographic findings. Orthop J Sports Med 2014;2:2325967114545298. https://doi.org/10.1177/2325967114545298.
20. Matsuura T, Suzue N, Kashiwaguchi S, Arisawa K, Yasui N. Elbow injuries in youth baseball players without prior elbow pain: A 1-year prospective study. Orthop J Sports Med 2013;1:2325967113509948. https://doi.org/10.1177/2325967113509948.
21. Matsuura Y, Kuniyoshi K, Suzuki T, Ogawa Y, Sukegawa K, Rokkaku T, et al. Accuracy of specimen-specific nonlinear finite element analysis for evaluation of distal radius strength in cadaver material. J Orthop Sci 2014;19:1012-8. https://doi.org/10.1007/s00776-014-0616-1.
22. Matsuyama K, Ishidou Y, Guo YM, Kakoi H, Setoguchi T, Nagano S, et al. Finite element analysis of cementless femoral stems based on mid- and long-term radiological evaluation. BMC Musculoskelet Disord 2016;17:397. https://doi.org/10.1186/s12891-016-1260-z.
23. Miguel-Andres I, Alonso-Rasgado T, Walmsley A, Watts AC. Effect of anconeus muscle blocking on elbow kinematics: Electromyographic, inertial sensors and

finite element study. Ann Biomed Eng 2017;45:775-88. https://doi.org/10.1007/s10439-016-1715-2.

24. Mihata T, Quigley R, Robicheaux G, McGarry MH, Neo M, Lee TQ. Biomechanical characteristics of osteochondral defects of the humeral capitellum. Am J Sports Med 2013;41:1909-14. https://doi.org/10.1177/0363546513490652.

25. Millard N, DeMoss A, McIlvain G, Beckett JA, Jasko JJ, Timmons MK. Wrist flexion exercise increases the width of the medial elbow joint space during a valgus stress test. J Ultrasound Med 2019;38:959-66. https://doi.org/10.1002/jum.14779.

26. Miura M, Nakamura J, Matsuura Y, Wako Y, Suzuki T, Hagiwara S, et al. Prediction of fracture load and stiffness of the proximal femur by CT-based specimen specific finite element analysis: cadaveric validation study. BMC Musculoskelet Disord 2017;18:536. https://doi.org/10.1186/s12891-017-1898-1.

27. Miyamura S, Oka K, Abe S, Shigi A, Tanaka H, Sugamoto K, et al. Altered bone density and stress distribution patterns in long-standing cubitus varus deformity and their effect during early osteoarthritis of the elbow. Osteoarthritis Cartilage 2018;26:72-83. https://doi.org/10.1016/j.joca.2017.10.004.

28. Momma D, Iwasaki N, Oizumi N, Nakatsuchi H, Funakoshi T, Kamishima T, et al. Long-term stress distribution patterns across the elbow joint in baseball players assessed by computed tomography osteoabsorptiometry. Am J Sports Med 2011;39:336-41. https://doi.org/10.1177/0363546510383487.

29. Morrey BF. Applied anatomy and biomechanics of the elbow joint. Instr Course Lect 1986;35:59-68.

30. Murray TA, Cook TD, Werner SL, Schlegel TF, Hawkins RJ. The effects of extended play on professional baseball pitchers. Am J Sports Med 2001;29:137-42.

31. Oliveira JM. In: Reis RL, editor. Regenerative strategies for the treatment of knee joint disabilities. Cham: Springer International Publishing AG; 2017. ISBN: 9783319447834.

32. Otoshi K, Kikuchi S, Kato K, Sato R, Igari T, Kaga T, et al. Age-specific prevalence and clinical characteristics of humeral medial epicondyle apophysitis and osteochondritis dissecans: Ultrasonographic assessment of 4249 players. Orthop J Sports Med 2017;5:2325967117707703. https://doi.org/10.1177/2325967117707703.

33. Park MC, Ahmad CS. Dynamic contributions of the flexor-pronator mass to elbow valgus stability. J Bone Joint Surg Am 2004;86:2268-74. https://doi.org/10.2106/00004623-200410000-00020.

34. Ruchelsman DE, Hall MP, Youm T. Osteochondritis dissecans of the capitellum: current concepts. J Am Acad Orthop Surg 2010;18:557-67. https://doi.org/10.5435/00124635-201009000-00007.

35. Schenck RC Jr, Athanasiou KA, Constantinides G, Gomez E. A biomechanical analysis of articular cartilage of the human elbow and a potential relationship to osteochondritis dissecans. Clin Orthop Relat Res 1994:305-12.

36. Sensini A, Cristofolini L. Biofabrication of electrospun scaffolds for the regeneration of tendons and ligaments. Materials (Basel) 2018;11:1963. https://doi.org/10.3390/ma11101963.

37. Takahara M, Mura N, Sasaki J, Harada M, Ogino T. Classification, treatment, and outcome of osteochondritis dissecans of the humeral capitellum. J Bone Joint Surg Am 2007;89:1205-14. https://doi.org/10.2106/00004623-200706000-00007.

38. Takahara M, Ogino T, Takagi M, Tsuchida H, Orui H, Nambu T. Natural progression of osteochondritis dissecans of the humeral capitellum: initial observations. Radiology 2000;216:207-12.

39. Takatori K, Hashizume H, Wake H, Inoue H, Nagayama N. Analysis of stress distribution in the humeroradial joint. J Orthop Sci 2002;7:650-7. https://doi.org/10.1007/s007760200116.